Experimental studies on a closed cycle demonstration OTEC plant working on small temperature difference

Mohammed Faizal, M. Rafiuddin Ahmed*

Division of Mechanical Engineering, The University of the South Pacific, Laucala Campus, Suva, Fiji Islands

Abstract

Ocean thermal energy conversion (OTEC) technology utilizes the temperature difference between the warm surface water and deep cold water of the ocean to operate a heat engine to generate electricity. An experimental study was carried out on a newly designed closed cycle demonstration OTEC plant with the help of temperature and pressure readings before and after each component. An increase in the warm water temperature increases the heat transfer between the warm water and the working fluid, thus increasing the working fluid temperature, pressure, and enthalpy before the turbine. The performance is better at larger flowrates of the working fluid and the warm water. It is found that the thermal efficiency and the power output of the system both increase with increasing operating temperature difference (difference between warm and cold water inlet temperature). Increasing turbine inlet temperatures also increase the efficiency and the work done by the turbine. The efficiency and the power output increase with increasing ratio of warm water to cold water flowrates. A maximum efficiency of about 1.5 % was achieved in the system. The findings from this work can contribute to the development of OTEC technologies.

Keywords: Ocean thermal energy conversion (OTEC); Closed cycle OTEC; thermal efficiency; demonstration OTEC plant

Nomenclature

eta	thermal efficiency
h	enthalpies
$\dot{V}_{CS}$	flowrate of cold water, L/s
$\dot{V}_{WF}$	flowrate of working fluid, L/s
$\dot{V}_{WS}$	flowrate of warm water, L/s
P	pressures (kPa)
T_{wsi}	warm water temperature at inlet of evaporator, ºC
T_{wso}	warm water temperature at outlet of evaporator, ºC
T_{csi}	cold water temperature at inlet of condenser, ºC
T_{cso}	cold water at outlet of condenser, ºC

1. Introduction

An ocean thermal energy conversion (OTEC) plant is basically a heat engine that utilizes the temperature difference between the warm surface water and deep cold sea water to drive a turbine to produce electricity, using the principles of a Rankine cycle [1]. A closed cycle OTEC system incorporates a working fluid operating between two heat exchangers in a closed cycle. A closed cycle utilizes the warm surface water to vaporize the working fluid in an evaporator. The vaporized fluid drives a turbine coupled to a generator. The vapor is then condensed in the condenser using cold deep seawater pumped to the surface. The condensed working fluid is pumped back to the evaporator and the cycle is repeated. Figure 1 shows a schematic diagram of a closed cycle OTEC plant [2].

The low temperature and pressure drop across the turbine is associated with the production of mechanical work. In practical operation of an OTEC power system, the gross power efficiency is only about half the Carnot limit. This reduces the maximum practical efficiency of OTEC gross power production to 3.5 - 4.0% [3].

Ocean thermal energy conversion plants are more suitable for low latitudes (tropical oceans) because the surface water temperature remains almost uniform throughout the year with few variations due to seasonal effects [4]. About 63% of the surface of the tropics between latitudes 30ºN and 30ºS is occupied by ocean water [5]. Solar energy that is absorbed by the tropical oceans maintains a relatively stable surface temperature of 26-28ºC to a depth of approximately 100 m. As the depth increases, the temperature drops, and at depths close to 1000 m, the

temperature is as low as 4ºC. Below this depth, the temperature drops only a few degrees. The temperature difference between warm and cold waters is maintained throughout the year with very few variations [3]. Pacific Island countries have a lot of potential for implementation of OTEC technologies because of the high ocean temperature gradient. Apart from generating electricity and producing fresh water, OTEC plants can be utilized for other benefits such as production of fuels such as hydrogen, ammonia, methanol, providing air-conditioning for buildings, on-shore and near-shore mariculture, and extraction of minerals [6,7,8].

2. Background

A lot of research work has been carried out on OTEC since its discovery in 1881. The first ever OTEC plant that was successfully commissioned was in Hawaii in 1979. A 50 kW closed cycle floating demonstration plant was constructed offshore. Cold water at a temperature of 4.4 °C was drawn from a depth of 670 m. During actual operation of the plant, it was found that biofouling, effects of mixing the deep cold water with the warm surface water, and debris clogging did not have any negative effects on plant operation. The longest continuous operation was for 120 hours [9]. A 100 kW OTEC pilot plant was constructed on-land for demonstration purposes in the republic of Nauru in October 1981 by Japan. The system operated between the warm surface water and a cold water source of 5-8°C at a depth of 500-700 m, with a temperature difference of 20°C [10]. The tests done were load response characteristics, turbine, and heat exchanger performance tests. The plant had operated by two shifts with one spare shift, and a continuous power generation record of ten days was achieved. The plant produced 31.5 kW of OTEC net power during continuous operation and was connected to the main power system [10].

A land based open cycle OTEC experimental plant was installed in Hawaii in 1993. The turbine-generator was designed for an output of 210 kW for 26 °C warm surface water and 6 °C deep water temperature. The highest gross power achieved was 255 kWe with a corresponding net power of 103 kW and 0.4 L/s of desalinated water [11]. Saga University, Japan, is actively involved in OTEC research and its byproduct studies. Experimental studies have been conducted on heat exchangers and on spray-flash evaporation desalination. Other studies done are on mineral water production using deep cold water, lithium extraction from seawater, hydrogen production, air-conditioning and aquaculture applications using deep cold water, and using the deep cold water for food processing and medical (cosmetic) applications [10].

Uehara et al. [12] presented a conceptual design for an OTEC plant in the Philippines after taking extensive temperature readings to determine a suitable site. The ocean surface water had a temperature range of 25 to 29ºC

throughout the year while the cold water remained between 4 to 8 ºC at a depth of 500 – 700 m. A total of 14 sites were suggested. A conceptual design for a 5 MW onland-type and a 25 MW floating-type were computed for. After doing cost estimates of the proposed systems, the construction of the 5 MW onland-type plant was suggested.

Uehara and Ikegami [2] performed an optimization study of a closed cycle OTEC system. They presented numerical results for a 100 MW OTEC plant with plate heat exchangers and ammonia as the working fluid. They concluded that the net power can reach upto 70.3% of the gross power of 100 MW for inlet warm water temperature of 26 ºC and inlet cold water temperature of 4 ºC. Yeh et al. [13] conducted a theoretical investigation on the effects of the temperature and flowrate of cold sea water on the net output of an OTEC plant. They found out that the maximum net output exists at a certain flowrate of the cold seawater. The output is higher for a larger ratio of warm to cold seawater flowrate.

Uehara et al. [14] did a performance analysis of an integrated hybrid OTEC plant. The plant is a combination of a closed cycle OTEC plant and a spray flash desalination plant. The total heat transfer area of the heat exchangers per net power is used as an objective function. A numerical analysis was done for a 10 MW integrated hybrid plant. Straatman and Sark [15] proposed a new hybrid OTEC with an offshore solar pond to optimize costs of electricity. This proposed system would increase the OTEC efficiency from 3% to 12%. The addition of a floating offshore solar pond to an OTEC system increases the temperature difference in the Rankine cycle, which is the cycle OTEC operates on.

Yamada et al. [16] did a performance simulation of a solar-boosted ocean thermal energy conversion plant, termed as SOTEC. The temperature of warm sea water used in the evaporator was increased by using a solar thermal collector. The simulation results showed that the proposed SOTEC plant can increase the overall efficiency of the OTEC system. Tong et al. [17] proposed a solar energy reheated power cycle to improve performance. They suggested that a solar collector introduced at the evaporator will greatly improve the temperature difference and thus the cycle performance. Also, it was found that without any additional loadings on the heat exchangers, increasing the turbine inlet pressure will also improve the OTEC system performance. Ganic and Wu [18] analyzed the effect of three working fluids used in OTEC. The fluids studied were ammonia, propane, and Freon-114. Seven different combinations of shell-and-tube heat exchangers were considered and for each combination, a computer model of the OTEC system was used. The comparisons were made based on the total heat transfer area of the heat exchangers divided by the net power output of the plant. It was found that Ammonia was the best fluid because of its relatively high thermal conductivity. Kim et al. [19] did a numerical analysis for

the same conditions but with various working fluids for a closed system, a regeneration system, an open system, a Kalina system, and a hybrid system. They concluded that the regeneration system using R125 as the working fluid had better performance. They also found that using the condenser effluent of a nuclear power plant rather than ocean surface water increased the system efficiency by approximately 2%.

Kazim [20] did studies on hydrogen production through an OTEC system. A technical analysis was done on an OTEC system coupled with a polymer electrolyte membrane electrolyser. The results demonstrated the significance of temperature drop and temperature difference on the electrical power output and conversion efficiency. Moore and Martin [21] presented a general mathematical framework for the synthesis of OTEC power generating systems. They developed a systematic methodology which was demonstrated in an OTEC system with ammonia as the working fluid. The power generated was used to drive a proton exchange membrane (PEM) electrolyser for hydrogen production. Faizal and Ahmed [22] performed experimental studies on corrugated plate heat exchangers for small temperature applications. They varied the channel spacing. They found that the minimum channel spacing gave optimal heat transfer. Guo-Yan et al. [23] presented a techno-economic study on compact heat exchangers to choose an optimum heat exchanger with minimum pressure drop. They concluded that all compact heat exchangers are feasible from an energy point of view. However, the performance differs because of the materials used. Research on heat exchangers for use in OTEC plants have also been conducted in Saga University, Japan [3]. Together with a large pressure drop across the turbine, a high heat transfer rate between the working fluid and the ocean water in the heat exchangers is required for optimal power production in OTEC plants [3].

Nihous and Syed [16] presented a financing strategy for small land-based OTEC plants. It is based on the cost effectiveness of some OTEC by-products. The main aim of the financing strategy presented is that the by-products would gradually payback the huge amount of capital cost required to build a small OTEC plant. Faizal and Ahmed [24] presented a review on the ocean heat budget and ocean thermal energy conversion. The heat exchange processes in the ocean are represented in an ocean heat budget. The heat budget quantifies the amount of heat gained and lost by the ocean, and this can be used to determine the overall temperature change of the ocean. Ocean thermal energy conversion plants can alter the surface temperatures of the ocean, but this has not been faced so far in some of the operational demonstration OTEC plants.

The present work is aimed at building a lab-based demonstration OTEC plant that operates on small temperature differences. The performance of the system is studied at different operating conditions. The pressure drop across the turbine and the system efficiencies and power output are presented.

3. Experimental set-up and procedure

A closed cycle demonstration OTEC plant with refrigerant R134-a as the working fluid was designed, built and experimented on. R134-a was used because it is not flammable at the low operating pressure and temperature of the experimental OTEC system. Also, R134-a is one of the limited refrigerants that could be used in the refrigerant pump in the current setup. Figure 2 shows a schematic of the demonstration plant. Figure 3 shows a photograph of the experimental setup.

Copper tubes with a total length of 5 m and external diameter of 15.88 mm (wall thickness = 1.24 mm) were used in the system. Pressure and temperature gauges were placed before and after each component of the system. MINGZHU pressure gauges (model: MZ-B9028), with an accuracy of 1%, were used to record pressure changes. The high side gauge has a pressure range of 0 – 3447 kPa and the low side gauge has a pressure range of 0 – 1517 kPa. CABA`C T6201 digital thermometers, with a resolution of 0.1 ºC and a temperature range of -50 ºC to +250 ºC were used to record the temperature. A storage tank with a capacity of 6 liters is placed just before the refrigerant pump to ensure that the pump receives a continuous supply of refrigerant and is not starved. A National Refrigeration Products LP22E refrigerant pump was used to circulate the working fluid (R134-a) in the system. This is a gear pump with a capacity of 0.15 kg/s with a power rating of 372.8 W. A voltage regulator was used to vary the pump rpm to regulate the working fluid flowrate. A GPI commercial grade flowmeter (model: A109A025LM low flow Aluminum flowmeter) with a flow range of 1 – 11 L/min was installed between the pump and evaporator to record the flowrate of the working fluid.

The water pumps used to pump warm and cold waters through the heat exchangers are centrifugal pumps (model: CP200SN) with a power rating of 550 Watts, flow of 130 L/min, and a head of 23 meters. Shut valves were used to control the flowrate. Both the warm and cold water were at atmospheric pressure. The temperature of the water at inlet and outlet of the heat exchangers were recorded using CABAC T6201 digital thermometers, with a resolution of 0.1 ºC and a temperature range of -50 ºC to +250 ºC. The warm water temperatures were 24 ºC, 27 ºC, and 30 ºC. The cold water temperature was kept constant between 4.5–5 ºC. The warm water flowrates, $\dot{V}_{WS}$, were varied from 0.38 – 0.46 L/s. The cold water flowrate, $\dot{V}_{CS}$, was kept constant at 0.16 L/s. The working fluid flowrates, $\dot{V}_{WF}$, were 2.5 L/s and 4.5 L/s. The heat exchangers are shell and tube type with three tubes spiraled. The first tube outer diameter is 15.88 mm with a wall thickness of 1.24 mm and the other tubes have an outer

diameter of 9.52 mm and wall thickness of 0.89 mm. The shell diameter is 115 mm with a height of 560 mm. Both the warm and cold water enters the heat exchangers from the bottom. This allows the water to fully fill the shells for effective heat transfer and prevent the formation of hydraulic diameters. An eight bladed mini, impulse turbine with a diameter of 130 mm enclosed in a metal casing of diameter of 140 mm is used in the system. The turbine is used to study the pressure and enthalpy drop of the working fluid. The pressure and temperature values read from the gauges were fed into a program in the Engineering Equation Solver (EES). All the thermodynamic properties were calculated using EES which were then used to calculate the efficiency and the power output.

4. Results and discussions

The efficiency and power output were calculated using the enthalpy values from EES. The other properties calculated were density, saturation temperature, and quality. The power output was calculated using the enthalpy drop across the turbine multiplied by the working fluid flowrate. The thermal efficiency was calculated by dividing the enthalpy drop across the turbine by the enthalpy difference between the outlet and inlet of the evaporator.

Figures 4 and 5 show the thermal efficiencies and the power output of the plant against the difference between the warm and cold water inlet temperatures for varying $\dot{V}_{WS}$ and for both $\dot{V}_{WF}$ .It is generally seen that the thermal efficiency and the power output increases with increasing temperature difference. The results are presented against the temperature difference because it is an important parameter in choosing actual plant installation sites and system design. Optimum power will be produced when the total temperature difference is sufficient to promote heat transfer in the heat exchangers as well as to provide a pressure drop across the turbine [3]. The efficiencies are higher for higher $\dot{V}_{WS}$. There is more heat transfer in the evaporator at higher flowrates because the warm water continuously supplies heat energy to the working fluid without losing much energy through the length of the heat exchanger, thus more heat transfer to the working fluids and better turbine performance. Yamada et al. [16] presented similar trends in efficiencies against the operating temperature difference. Hettiarachichi et al. [25] also presented the efficiencies against the operating temperature difference and obtained similar trends. The efficiencies for $\dot{V}_{WF}$ = 4.5 L/s are higher compared to $\dot{V}_{WF}$ = 2.5 L/s. Higher $\dot{V}_{WF}$ leads to a higher pressure at the turbine inlet and reduces heat loss to the surrounding on the higher temperature side. The range of thermal efficiencies for $\dot{V}_{WF}$ = 2.5 L/s is 0.8 – 1.15% and 0.8 – 1.5% for $\dot{V}_{WF}$ = 4.5 L/s.

The work done by the turbine for both $\dot{V}_{WF}$ generally increases with increasing operating temperature

difference, and is higher for larger $\dot{V}_{WS}$. The turbine uses most of the energy from the working fluid to do work, and as a result there is a pressure drop across the turbine which leads to an enthalpy drop. The larger the pressure (and enthalpy drop) across the turbine, the more work is done by the turbine. The power output for $\dot{V}_{WF}$ = 4.5L/s is higher compared to $\dot{V}_{WF}$ = 2.5 L/s. A higher $\dot{V}_{WF}$ gives a higher pressure at the turbine inlet and thus a higher pressure and enthalpy drop across the turbine. The power output for $\dot{V}_{WF}$ = 2.5 L/s is between 5 – 6.8 W and 8.5 – 15.8 W for $\dot{V}_{WF}$ = 4.5 L/s.

Figure 6 shows the turbine inlet pressure and turbine pressure drop against operating temperature difference, for $\dot{V}_{WS}$ = 0.46 L/s and both the $\dot{V}_{WS}$. The inlet pressure and pressure drop increased as the operating temperature (difference between warm water and cold water inlet temperature) difference increased. For $\dot{V}_{WF}$ = 2.5 L/s, the maximum pressure at the turbine inlet was 551.58 kPa and after the condenser was 455.05 kPa, for a warm water inlet temperature of 30ºC. For $\dot{V}_{WF}$ = 4.5 L/s, the maximum pressure at the turbine inlet was 586.05 kPa and after the condenser pressure was 482.63 kPa, for the same warm water inlet temperature of 30ºC. Thus, it can be seen that the pressure at the evaporator and condenser increased with increasing warm water inlet temperatures. The variations in the $\dot{V}_{WS}$ did not affect the pressure.

Figures 7 and 8 show the thermal efficiencies and the power output against the pressure drop across the turbine, for both $\dot{V}_{WF}$. The pressure drop across the turbine achieved in this demonstration system is between 40 – 75 kPa. Even though the results are presented against the pressure drop, the superheat at the turbine inlet will make a significant difference in the system performance, since phase change in the cycle ideally occurs at constant pressure. The superheat in the present system for both the working fluid flowrates is between 4.3 – 6.09 ºC. Without any major focus on superheating (since very less deviation among all cases), it is seen that the thermal efficiencies increase with increasing pressure across the turbine. Higher warm water flowrate give higher efficiencies. Also, $\dot{V}_{WF}$ = 4.5 L/s has higher efficiencies compared to $\dot{V}_{WF}$ = 2.5 L/s. The power output increases with increasing pressure drop in a manner similar to the thermal efficiencies. However, the superheat at the turbine inlet will make a huge difference in actual systems. The higher values for $\dot{V}_{WS}$ and $\dot{V}_{WF}$ gives higher power. For $\dot{V}_{WF}$ = 4.5 L/s, there is a significant jump in the pressure drop across the turbine which leads to a sudden increase in the efficiency.

Figures 9 and 10 show the thermal efficiency and the power output against the turbine inlet temperature for all $\dot{V}_{WS}$ and both $\dot{V}_{WF}$. The temperature values at the inlet of the turbine in this demonstration system are similar to those of actual systems. The turbine inlet temperature, achieved after the working fluid passes through the evaporator, is higher for higher values of the warm seawater inlet temperature (because of the high heat transfer due to higher temperature difference between the working fluid and warm water). The efficiencies for both the cases increase with increasing turbine inlet temperature. The higher the inlet temperature (for a given pressure), the higher will be the superheat and the enthalpy, thus more energy available to drive the turbine. Tong et al. [17] and Hettiarachichi et al. [25] had achieved similar trends for efficiency against turbine inlet temperature. The higher efficiencies are obtained for $\dot{V}_{WF}$ = 4.5 L/s and for larger $\dot{V}_{WS}$. The power output increases with increasing turbine inlet temperature and has similar trends to those of the thermal efficiencies. There is more work done by the turbine when the turbine inlet temperature is higher. The power is higher for $\dot{V}_{WF}$ = 4.5 L/s and for larger $\dot{V}_{WS}$.

Figures 11 and 12 show the thermal efficiencies and the power output against the ratio of the water flowrates, $\dot{V}_{ws}/\dot{V}_{cs}$, for both $\dot{V}_{WF}$. Both the efficiency and the power increase with increasing $\dot{V}_{ws}/\dot{V}_{cs}$. The highest efficiency and power for both $\dot{V}_{WF}$ are obtained for the maximum water temperature of 30ºC. The higher flowrate of the working fluid ($\dot{V}_{WF}$ = 4.5 L/s) gives higher efficiencies and power output. Yeh et al. [13] presented similar trends of the net work against the ratio of the water flowrates. They had also stated that it is always economical to increase the warm water flowrates since the pipe length of the warm water pipes are much smaller than the cold water pipes.

5. Conclusions

A closed cycle OTEC demonstration plant was designed and built to experimentally study its performance with the help of temperature and pressure readings before and after each component. A higher warm water temperature increases the heat transfer between the warm water and the working fluid, thus increasing the working fluid temperature, pressure, and enthalpy before the turbine. The performance is better at larger flowrates of the working fluid and the warm water. It is found that the thermal efficiency of the system and the work done by the turbine both increases with increasing operating temperature difference (difference between warm and cold water inlet temperature). The turbine inlet pressure and the pressure drop across the turbine both increase with increasing

operating temperature difference. Assuming constant superheating at turbine inlet, the performance of the system improves with increasing pressure drop across the turbine. Increasing turbine inlet temperatures also increase the efficiency and the work done by the turbine. The efficiency and the power output increase with increasing ratio of warm water flowrate to cold water flowrate. The results from this work can give more insight into the operational aspects of actual OTEC systems.

References

1. Lavi A. Ocean thermal energy conversion: a general introduction. Energy 1980; 5: 469-480.
2. Uehara H, Ikegami Y. Optimization of a closed-cycle OTEC system. Trans ASME Journal of Solar Energy Engineering 1990; 112:112–256.
3. Avery WH, Wu C. Renewable Energy from the Ocean—A Guide to OTEC. Oxford University Press: Oxford, 1994; 1–367.
4. Pelc P, Fujita RM. Renewable energy from the ocean. Marine Policy 2002; 26:471–479.
5. Magesh R. OTEC technology—a world of clean energy and water. In: Proceedings of the World Congress on Engineering 2010 Vol II WCE 2010, London UK, 2010.
6. Huang JC, Krock HJ, Oney SK. Revisit ocean thermal energy conversion system. Mitigation and Adaptation Strategies for Global Change 2003; 8:157–175.
7. National Renewable Energy Laboratory. Ocean thermal energy conversion—benefits of OTEC. Available from: http://www.nrel.gov/otec/benefits.html. Accessed on: 03.01.2012.
8. Tanner D. Ocean thermal energy conversion: current overview and future outlook. Renewable Energy 1995; Vol. 6 No. 3: 367-373.
9. McHale A, Jones W L, Horn HM. Deployment and operation of the 50kW mini-OTEC plant, OTC 3686. Offshore technology conference, Houston, 1980.
10. Mitsui T, Ito F, Seya Y, Nakamoto Y. Outline of the 100kW OTEC pilot plant in the republic of Nauru. IEE transactions on power apparatus and systems 1983; PAS-102:3167–3171.
11. Nihous GC, Syed MA, Vega LA. Conceptual design of an open cycle OTEC plant for the production of electricity and fresh water in a Pacific Island. In: Proceedings of the First International Conference on Ocean Energy Recovery ICOER, American Society of Civil Engineers, 1989.
12. Uehara H, Dilao CO, Nakaoka T. Conceptual design of ocean thermal energy conversion (OTEC) power plants in the Philippines. Solar Energy 1988; 41:431–441.

13. Yeh RH, Su TZ, Yang MS. Maximum output of an OTEC power plant. Ocean Engineering 2005; 32:685–700.
14. Uehara H, Miyara A, Ikegami Y, Nakaoka T. Performance analysis of an OTEC plant and a desalination plant using an integrate hybrid cycle. Trans ASME Journal of Solar Energy Engineering 1996; 118:115–122.
15. Straatman PJT, Sark WGJHM. A new hybrid ocean thermal energy conversion-offshore solar pond (OTEC-OSP) design: a cost optimization approach. Solar Energy 2008; 82:520–527.
16. Yamada N, Hoshi A, Ikegami Y. Performance simulation of solar-boosted ocean thermal energy conversion plant, Renewable Energy, 2009; 34 (7): 1752-1758, ISSN 0960-1481, 10.1016/j.renene.2008.12.028.
17. Tong W, Liang D, Chuangang GU, Bo Y. Performance analysis and improvement for CC–OTEC system. Journal of Mechanical Science and Technology 2008; 22:1977–1983.
18. Ganic EN, Wu J. On the selection of working fluids for OTEC power plants, Energy Conversion and Management 1980; 20 (1): 9-22, ISSN 0196-8904, 10.1016/0196-8904(80)90024-2.
19. Kim NJ, Ng KC, Chun W. Using the condenser effluent from a nuclear power plant for ocean thermal energy conversion (OTEC). International Communications in Heat and Mass Transfer 2009; 36:1008–1013.
20. Kazim A. Hydrogen production through an ocean thermal energy conversion system operating at an optimum temperature drop. Applied Thermal Engineering 2005; 25 (14-15): 2236-2246.
21. Moore FP, Martin LL. A nonlinear nonconvex minimum total heat transfer area formulation for ocean thermal energy conversion (OTEC) systems, Applied Thermal Engineering 2008; 28(8-9): 1015-1021, ISSN 1359-4311, 10.1016/j.applthermaleng.2007.06.039.
22. Faizal M, Ahmed MR. Experimental studies on a corrugated plate heat exchanger for small temperature difference applications, Experimental Thermal and Fluid Science 2012; 36: 242-248, ISSN 0894-1777, 10.1016/j.expthermflusci.2011.09.019.
23. Guo-Yan Z, En W, Shan-Tung T. Techno-economic study on compact heat exchangers. International Journal of Energy Research 2008; 32:1119–1127.
24. Faizal, M Ahmed MR. On the ocean heat budget and ocean thermal energy conversion. International Journal of Energy Research 2012; 35: 1119–1144. doi: 10.1002/er.1885
25. Hettiarachichi HD, Golubovic M, Worek WM, Ikegami Y. Optimum design criteria for an organic Rankine cycle using low-temperature geothermal heat sources 2007; 32: 1698-1706.

Figure 1

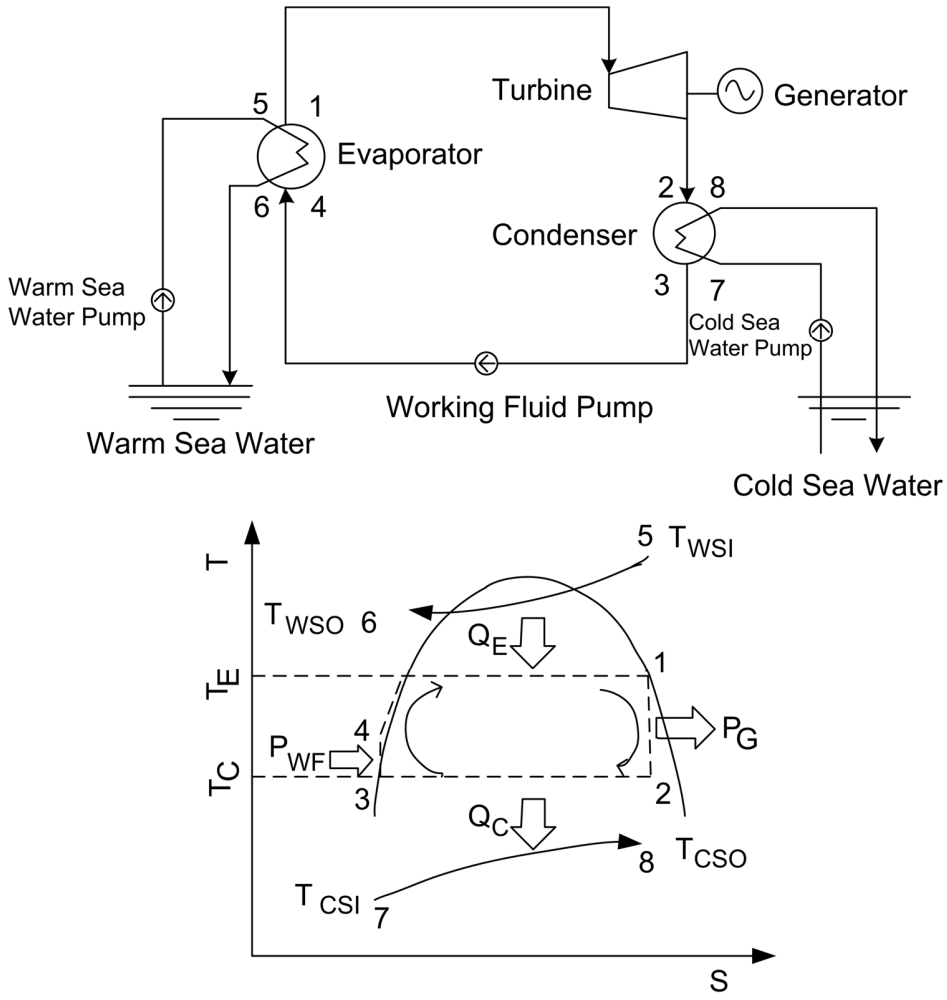

Fig. 1. Schematic diagram of a closed cycle OTEC plant [2].

Figure 2

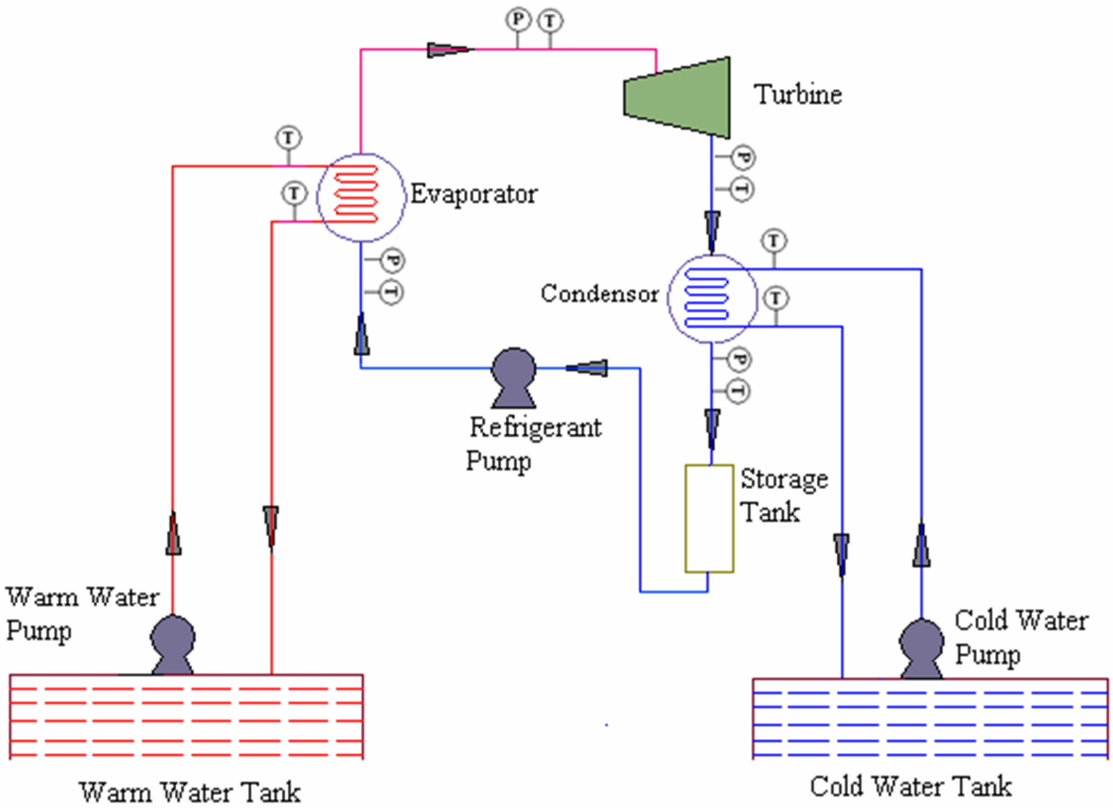

Fig. 2. Schematic diagram of the OTEC demonstration plant (P = pressure gauges, T = Temperature sensors).

Figure 3

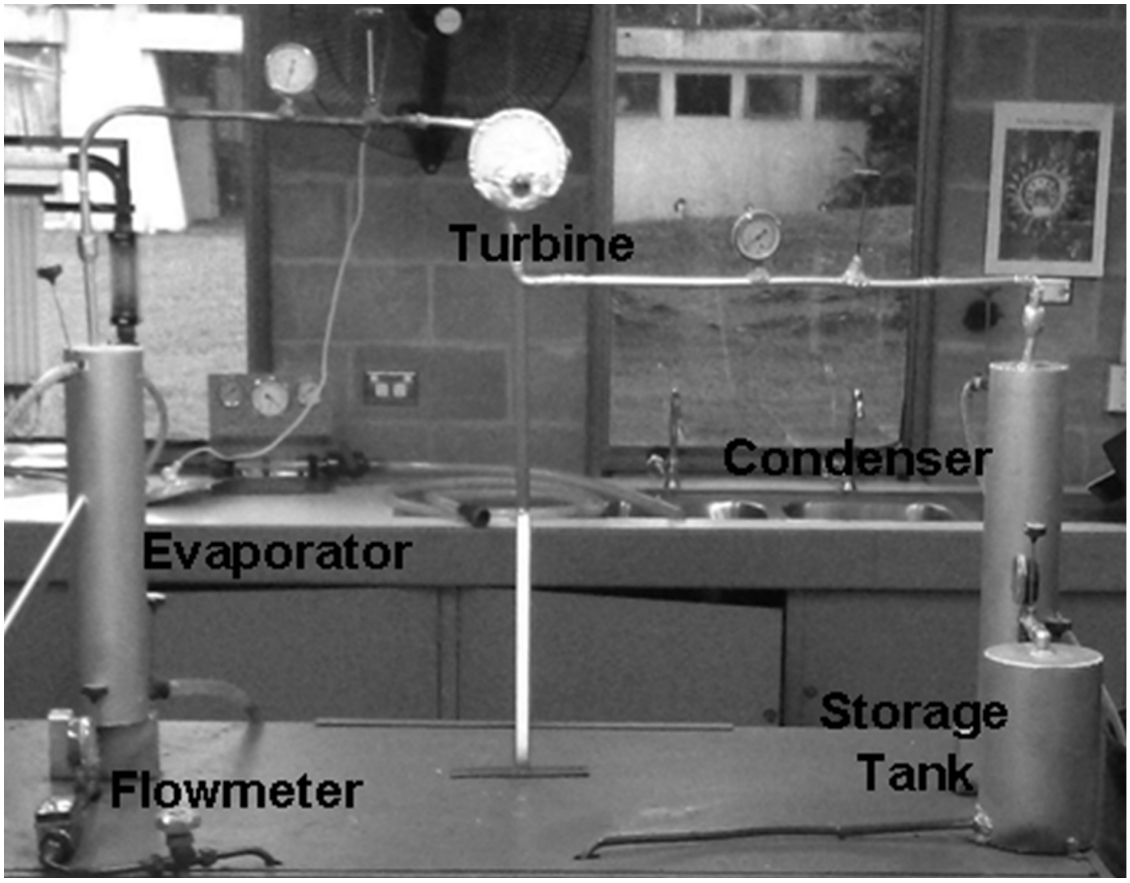

Fig. 3. A photograph of the experimental setup.

Figure 4

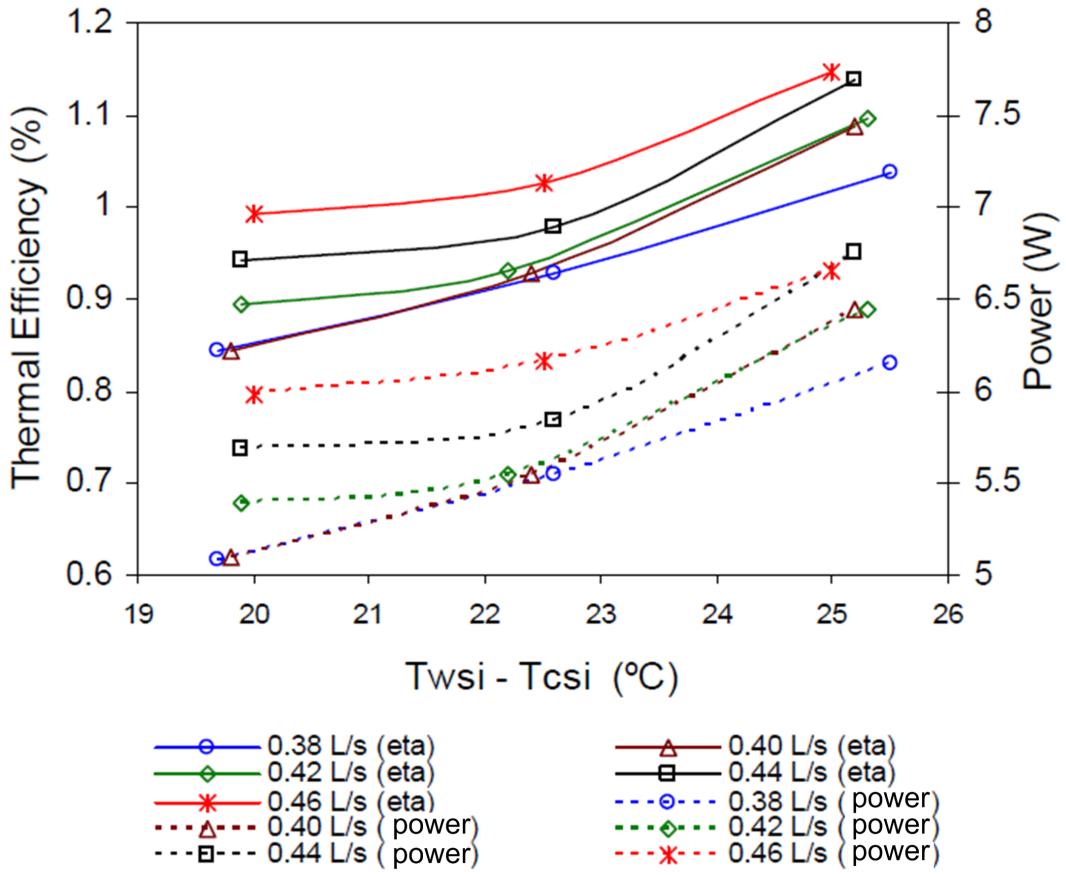

Fig. 4. Thermal efficiency and power output of the system against operating temperature difference, for $\dot{V}_{WF}$ = 2.5 L/s, and varying $\dot{V}_{WS}$.

Figure 5

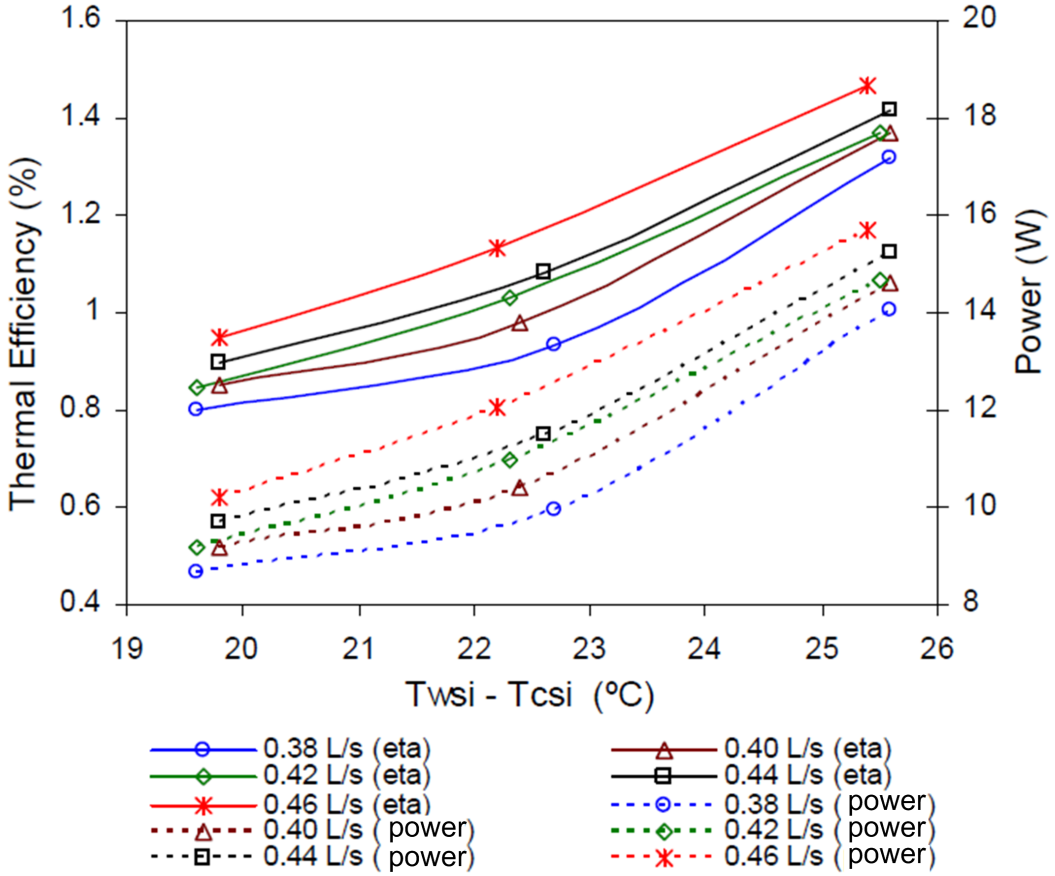

Fig. 5. Thermal efficiency and power output of the system against operating temperature difference, for $\dot{V}_{WF}$ = 4.5 L/s, and varying $\dot{V}_{WS}$.

Figure 6

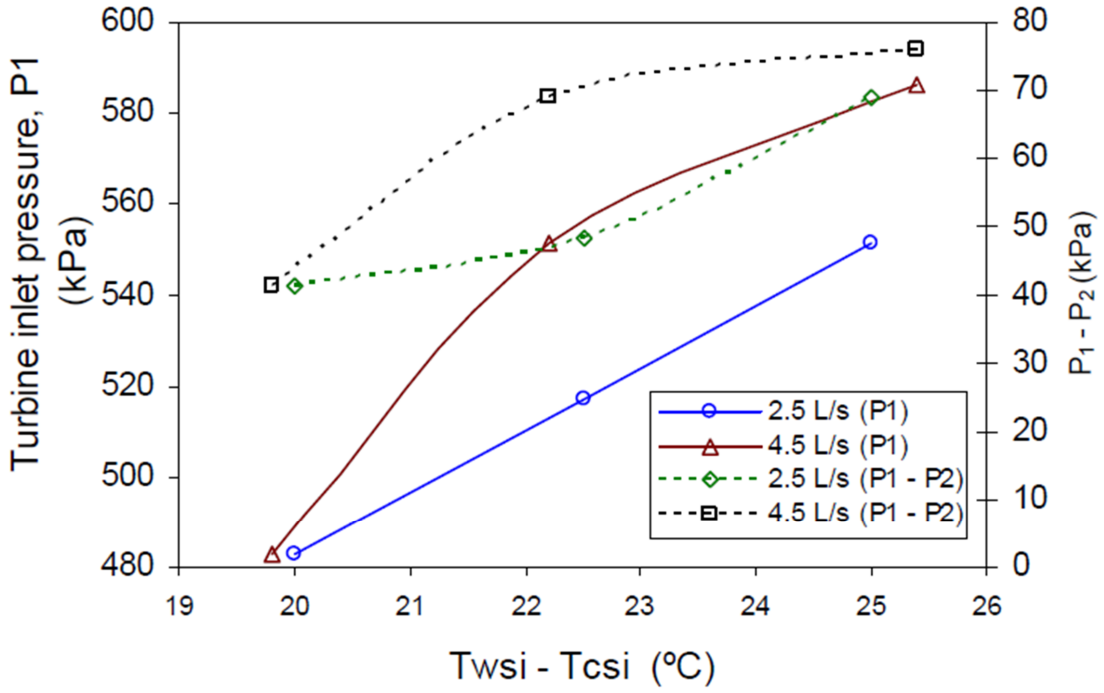

Fig. 6. Turbine inlet pressure and turbine pressure drop against operating temperature difference, for $\dot{V}_{WS}$ = 0.46 L/s and both the $\dot{V}_{WF}$.

Figure 7

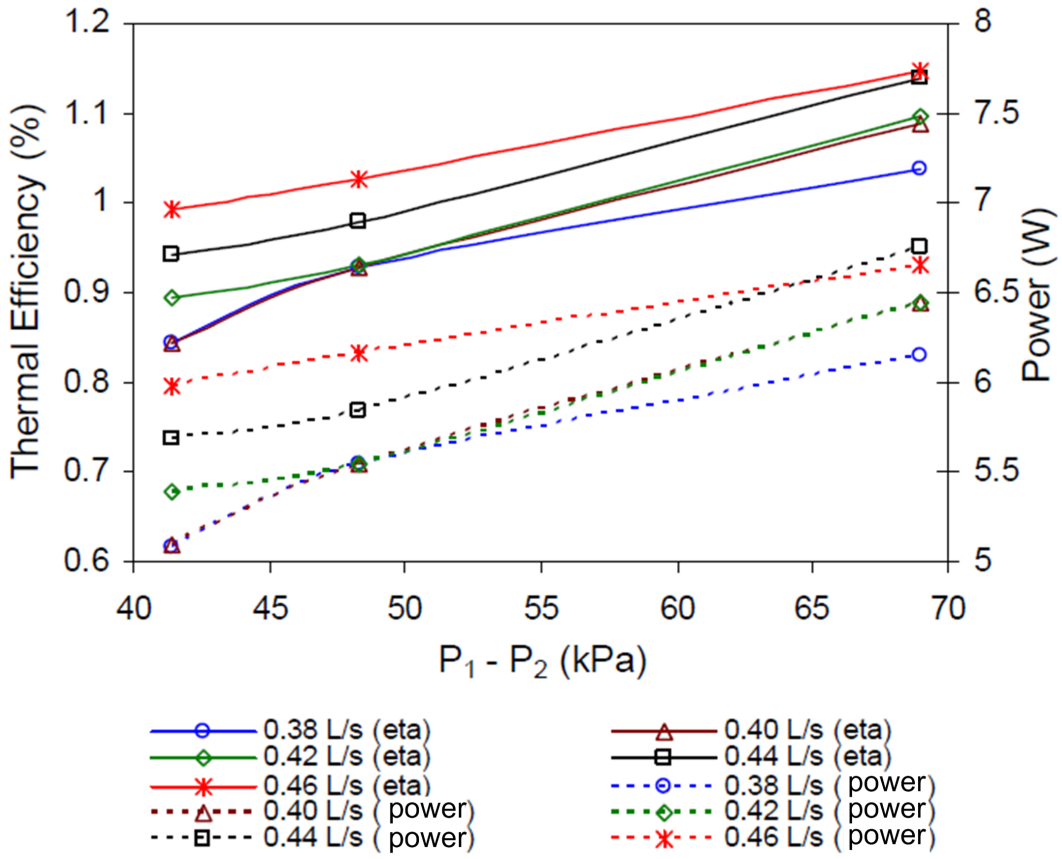

Fig. 7. Thermal efficiency and power output of the system against the pressure drop across the turbine, for $\dot{V}_{WF}$ = 2.5 L/s and varying $\dot{V}_{WS}$.

Figure 8

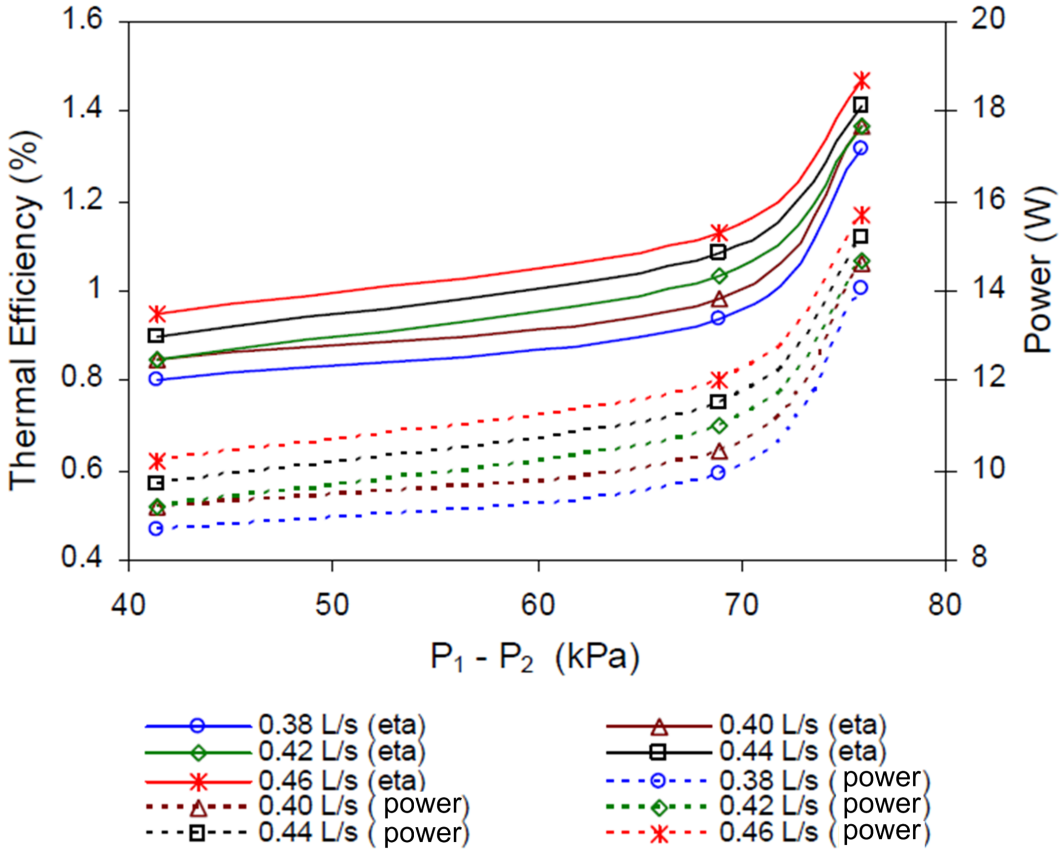

Fig. 8. Thermal efficiency and power output of the system against the pressure drop across the turbine, for $\dot{V}_{WF}$ = 4.5 L/s and varying $\dot{V}_{WS}$.

Figure 9

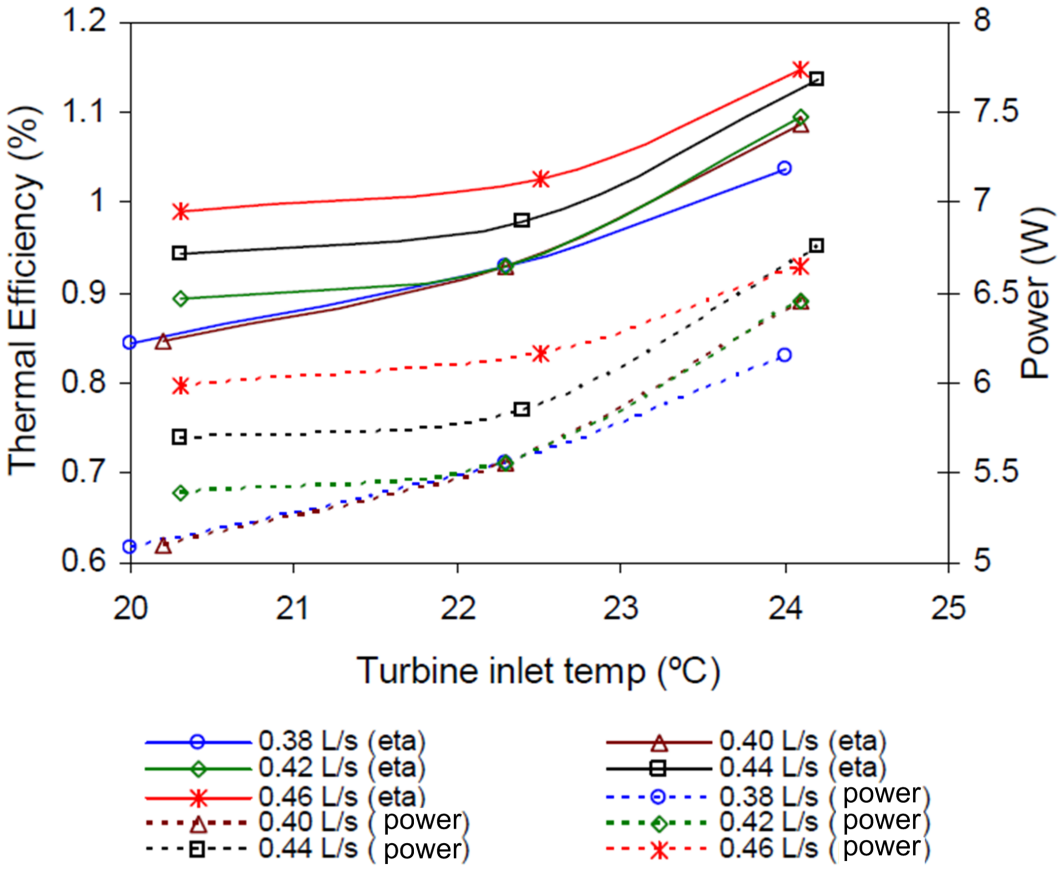

Fig. 9. Thermal efficiency and power output of the system against turbine inlet temperature, for $\dot{V}_{WF}$ = 2.5 L/s and varying $\dot{V}_{WS}$.

Figure 10

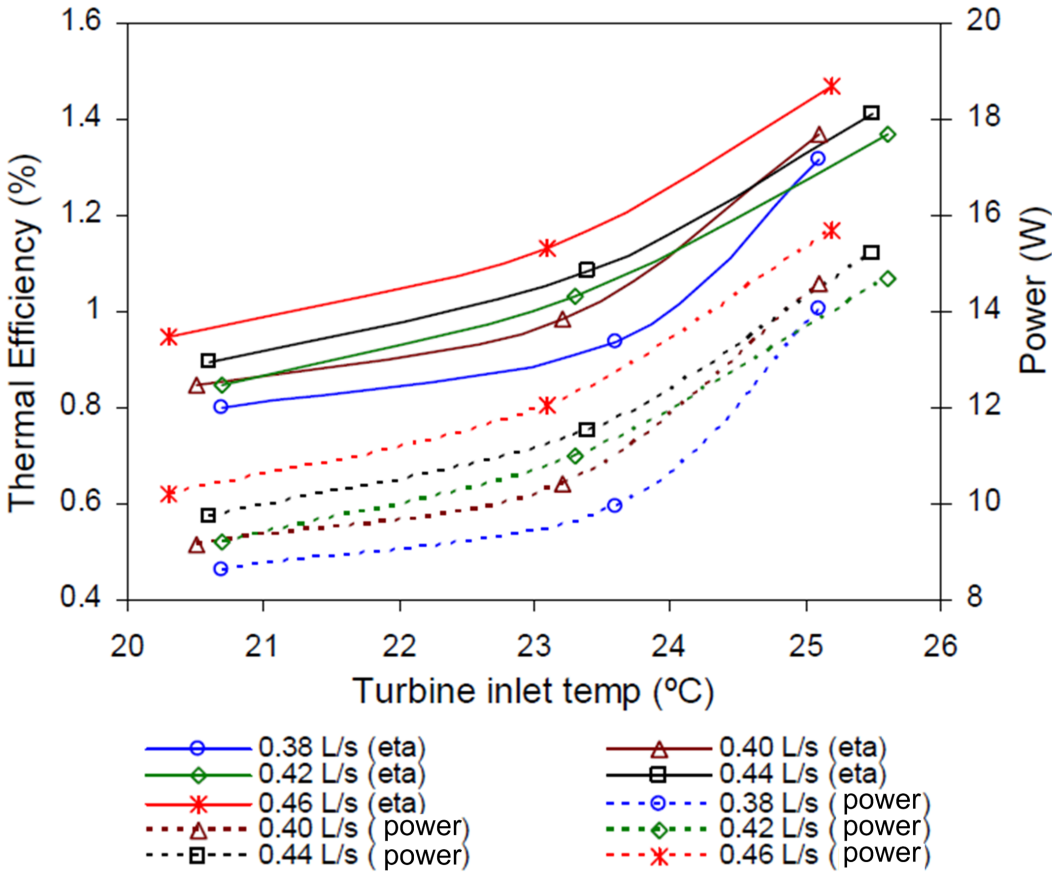

Fig. 10. Thermal efficiency and power output of the system against turbine inlet temperature, for $\dot{V}_{WF}$ = 4.5 L/s and varying $\dot{V}_{WS}$.

Figure 11

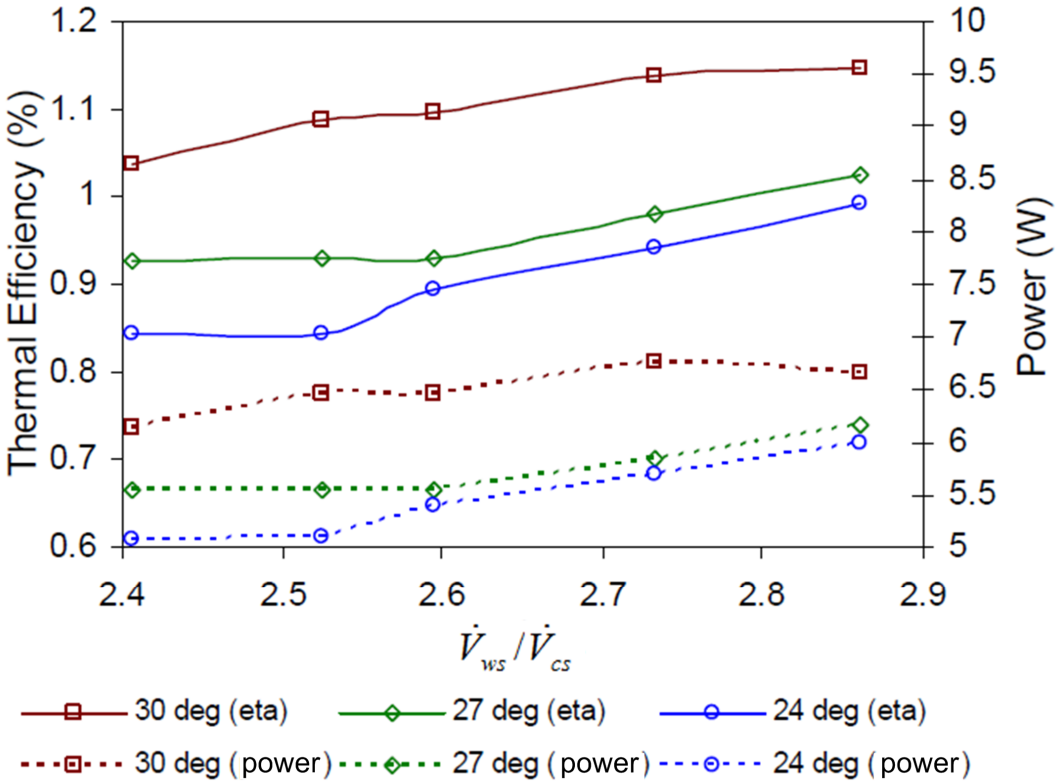

Fig. 11. Thermal efficiency and power output of the system against the ratio of the water flowrates, $\dot{V}_{ws}/\dot{V}_{cs}$, for $\dot{V}_{WF}$ = 2.5 L/s and all warm water temperatures.

Figure 12

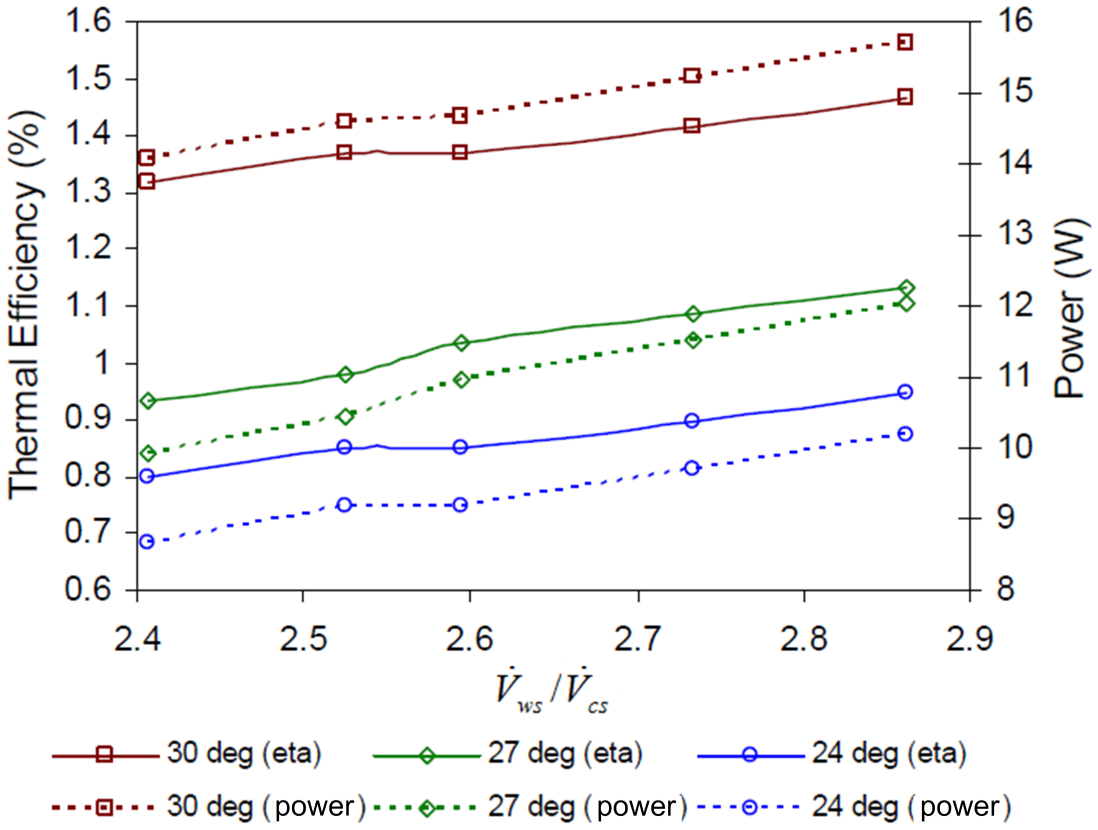

Fig. 12. Thermal efficiency and power output of the system against the ratio of the water flowrates, $\dot{V}_{ws}/\dot{V}_{cs}$, for $\dot{V}_{WF}$ = 4.5 L/s and all warm water temperatures.